Journal of Inflammation Research

Dovepress
Taylor & Francis Group

Open Access Full Text Article

ORIGINAL RESEARCH

Saikosaponin-d Attenuates Irinotecan-Induced Intestinal Toxicity via TAK1/NF-κB Pathway and Enhances Antitumor Efficacy

Peng Zheng[1,2,*], Rui Ma[1,3,*], Xiaoya Liu[2], Luda Song[3], Bing Ma[1,*], Guijun Zou[1,*]

[1]Department of General Surgery, The First Medical Center of Chinese PLA General Hospital, Beijing, 100853, People's Republic of China; [2]Department of General Surgery, The Sixth Medical Center of Chinese PLA General Hospital, Beijing, 100048, People's Republic of China; [3]Medical School of Chinese PLA, Beijing, People's Republic of China

*These authors contributed equally to this work

Correspondence: Bing Ma; Guijun Zou, Department of General Surgery, The First Medical Center of Chinese PLA General Hospital, Beijing, 100853, People's Republic of China, Email mabingcaowei1983@sina.com; zougj301@163.com

Purpose: Saikosaponin-d (SSD), a bioactive triterpenoid saponin derived from Bupleurum species (a traditional Chinese medicine), is recognized for its gastrointestinal protective properties. This study investigates the therapeutic potential and mechanisms of SSD against irinotecan (IRI)-induced intestinal mucositis.

Methods: Using a CT26 colorectal cancer Syngeneic mouse model (BALB/c mice), we evaluated the synergistic antitumor efficacy of SSD combined with IRI. Concurrently, the protective effects of SSD against IRI-induced intestinal toxicity were assessed in vivo (BALB/c mice) and in vitro (lipopolysaccharide (LPS)-stimulated Caco-2 cells). In vivo evaluations included monitoring body weight changes, diarrhea severity, colon length, and histopathological alterations. Mechanistic insights into the anti-inflammatory and antioxidant effects were elucidated through RT-qPCR, Western blotting, immunohistochemistry, and oxidative stress marker analysis.

Results: SSD significantly mitigated IRI-induced intestinal injury, as demonstrated by attenuated body weight loss, improved diarrhea scores, and preserved colon length. Histopathological examination revealed that SSD protected intestinal epithelial integrity and enhanced barrier function. Mechanistically, SSD reduced oxidative stress by modulating antioxidant enzyme activities (SOD, GSH-Px) and suppressing lipid peroxidation (MDA levels). Furthermore, SSD inhibited proinflammatory cytokine production (IL-6, TNF-α, IL-1β) via downregulation of the TAK1/NF-κB pathway in both IRI-treated mice and LPS-challenged Caco-2 cells.

Conclusion: Our findings demonstrate that SSD alleviates IRI-induced intestinal mucositis through suppression of the TAK1/NF-κB signaling cascade, highlighting its potential as an adjuvant therapy to enhance the safety profile of IRI-based chemotherapy.

Keywords: intestinal mucositis, oxidative stress modulation, gastrointestinal protection, cytokine reduction, TAK1/NF-κB pathway

Introduction

Chemotherapeutic agents are widely used in cancer treatment, but their non-specific distribution and toxic side effects cause significant harm to non-cancerous tissues, limiting their clinical application.[1,2] Irinotecan (IRI), a water-soluble camptothecin derivative, is used in the treatment of colorectal cancer but can lead to severe intestinal toxicity, particularly delayed diarrhea.[3,4] Studies have indicated that the regeneration of non-toxic IRI or SN-38 glucuronides into toxic SN-38 in the intestine is a multifactorial process involving drug metabolism in the enterohepatic circulation, bacterial β-glucuronidase, the gut microbiota, the innate mucosal immune system, and intestinal tight junctions.[5–7] However, the precise mechanisms underlying IRI-induced intestinal toxicity remain incompletely understood. Current consensus posits that the intestinal accumulation of the toxic metabolite SN-38 induces epithelial cell damage and barrier dysfunction, thereby permitting luminal pathogens, toxins, undigested nutrients, and microbial products to activate immune cells as antigenic stimuli, ultimately driving pro-inflammatory cascades.[8] Notably, the intestinal toxicity of IRI can result in

Received: 8 November 2024
Accepted: 16 May 2025
Published: 18 June 2025

electrolyte imbalances, dehydration, severe pain, and even death in patients.[9] Therefore, current research focuses on finding effective adjuvant treatment strategies to mitigate the intestinal toxicity of IRI and enhance its anti-tumor efficacy.

In current medical practice, despite exploring various treatment strategies such as the use of Ganciclovir,[10] P-glycoprotein blockers,[11] and tumor necrosis factor-α inhibitors,[12] the therapeutic outcomes have not reached an ideal level, and this issue remains challenging to resolve. Traditional Chinese medicine has a longstanding history in the treatment of tumors, with numerous active components demonstrating potential anti-tumor effects while maintaining low toxicity.[13,14] Particularly noteworthy is the significant potential of certain herbal extracts and compounds in alleviating IRI-induced intestinal toxicity.[15] Among the most esteemed traditional Chinese herbs is Bupleurum, known for its diverse therapeutic benefits, including anti-inflammatory, anti-tumor, antimalarial, and antipyretic properties.[16–18] From the root of Bupleurum, various active components can be extracted, with Saikosaponin-d (SSD) being the most abundant. Research indicates that SSD possesses anti-inflammatory, anti-tumor, and antiviral effects through multiple mechanisms.[19,20] For instance, it can inhibit inflammasome activation and improve inflammatory conditions by promoting NLRP3 ubiquitination.[21] Additionally, SSD has been found to alleviate chemotherapy-induced neutropenia by activating the CBL-dependent ERK pathway.[22] Further studies report that SSD reduces ventilation-induced lung injury in rats by inhibiting pro-inflammatory cytokine expression, diminishing oxidative stress, and reducing apoptosis.[23] Moreover, SSD exhibits anti-cancer capabilities by inhibiting TNF-α-induced cancer cell invasion.[24] It is also validated to ameliorate cisplatin-induced nephrotoxicity by inhibiting ROS-mediated MAPK and NF-κB pathways.[25] Transforming Growth Factor Beta-Activated Kinase 1 (TAK1)/Nuclear factor kappa-B (NF-κB) signaling pathway is increasingly recognized as a crucial player in the inflammatory response in many diseases, as well as in chemotherapy-induced toxicities.[26–28]

Although studies have shown that SSD can alleviate chemotherapy-induced toxicities, its effects on IRI-induced colitis during colorectal cancer treatment have not yet been explored. We hypothesize that SSD alleviates IRI-induced toxicity by modulating the TAK1/NF-kB signaling pathway, thereby reducing inflammation and oxidative stress. This study aims to investigate the efficacy and mechanisms of SSD in reducing chemotherapy-related toxic reactions and enhancing anti-tumor activity, providing foundational data for its potential clinical application.

Materials and Methods

Reagents

Irinotecan (IRI, with a purity of ≥99%) was procured from Med Chem Express (MCE) Biotechnology Co., Ltd., located in Shanghai, China. SSD (with a purity of >98% and a molecular weight of 780.98 Da) was also sourced from Med Chem Express (MCE) Biotechnology Co., Ltd. The antibodies used for Western blot analysis, including ZO-1, Occludin-1, E-cadherin, and GAPDH, were supplied by Abclone Biotechnology Co., Ltd. in Beijing, China. Antibodies for TAK1, IkB-α, p-IkB-α, p65, and p-p65 were obtained from Wuhan Sanying Biotechnology Co., Ltd., Wuhan, China. The HRP-conjugated goat anti-rabbit secondary antibody was purchased from ZSGB-BIO Co., Ltd., also based in Beijing, China.

Cells and Animals (Ethical Statement)

Cells: Caco-2 colorectal adenocarcinoma cells (ProCell, CL-0050) were cultured in Minimum Essential Medium (MEM; Gibco, 11095080) supplemented with 20% fetal bovine serum (FBS; Gibco, 10091148). CT26 colorectal adenocarcinoma cells (ProCell, CL-0071) were maintained in Dulbecco's Modified Eagle Medium (DMEM; Gibco, 11965092) containing 10% FBS. All cells were incubated at 37°C in a humidified atmosphere with 5% CO_2.

Animals: Specific pathogen-free (SPF) female BALB/c mice (6–8 weeks old, body weight 18–25 g) were purchased from SPF Biotechnology Co., Ltd. (Beijing, China) and acclimatised for one week before the experiments. The mice were housed in individually ventilated cage (IVC) systems under controlled environmental conditions (temperature 23°C ± 2°C, humidity 55% ± 5%) with ad libitum access to sterilised standard rodent feed and water.

All experiments were conducted in strict accordance with the Guidelines for the Care and Use of Laboratory Animals. Ethical approval was obtained from the ethics committee of the Institute of Analysis and Testing, Beijing Academy of

Science and Technology (Approval Number: 240408-SWDWF-007). Animal welfare assessments followed the national standard Laboratory Animal-Guideline for Ethical Review of Animal Welfare (GB/T 35892-2018).

Mouse Subcutaneous Syngeneic Tumor Model

CT26 cells (2×10^6) were injected into the left flank of the mice. Once the tumors reached a volume of 50 mm^3, the mice with Syngeneic were randomly divided into one of four groups (day 0): control group, IRI group, low-dose SSD group, and high-dose SSD group. SSD was administered intraperitoneally every other day at doses of 4 mg/kg or 8 mg/kg for 11 days. The dosage of SSD was determined based on the study by Li et al investigating SSD's efficacy in alleviating Dextran Sulfate Sodium (DSS)-induced colitis.[29] Irinotecan (50 mg/kg) was injected intraperitoneally from days 8 to 11. No treatment was given to the mice on days 12 and 13. Tumor size was assessed every other day using calipers, and mice were weighed with a balance. Tumor volume was calculated using the formula: volume (mm^3) = (length × $width^2$) / 2. On day 14, mice were euthanized, and samples of tumors and intestinal tissues were collected for further analysis.

Mouse Model of IRI-Induced Intestinal Mucositis

The mouse model of IRI-induced Intestinal mucositis was established based on previous studies. Mice were intraperitoneally injected with 50 mg/kg IRI daily for four consecutive days. Mice exhibiting Intestinal mucositis symptoms were randomly divided into four groups, with three mice per group. Except for the untreated control group, the IRI pre-treated mice received intraperitoneal injections of SSD at doses of 4 mg/kg or 8 mg/kg once daily from days 1 to 11, and were referred to as L-SSD and H-SSD, respectively, based on the dosage. Mice not treated with IRI were used as the blank control group and were administered saline in the same manner as the experimental groups. From day 8, mice were intraperitoneally injected with IRI for four consecutive days. Body weight, stool consistency, food intake, and water consumption were recorded daily. On day 14, mice were euthanised with isoflurane for further experiments.

CCK-8 Cell Viability Assay

Caco-2 cells were seeded into 96-well plates at a density of 500 cells per well and treated with SSDat varying concentrations of 0.5, 1, 2.5, 5, 10, 20 and 40 μM for 24 hours. Following treatment, 10 μL of CCK-8 reagent (TargetMol, C0005) along with 90 μL of MEM was added to each well. The plates were then incubated at 37°C for 2 hours. Prior to measuring absorbance, the 96-well plates were gently shaken for 5 minutes. Cell viability was then quantitatively measured using a microplate reader set to 450 nm. All experiments were conducted in triplicate to ensure reliability of the results.

Oxidative Indicators

Using assay kits provided by the manufacturer, the levels of myeloperoxidase (MPO; Solarbio, BC5715), superoxide dismutase (SOD; Beyotime, S0101M), glutathione peroxidase (GSH-Px; Beyotime, S0057S), and malondialdehyde (MDA; Beyotime, S0131M) in colon tissue were assessed. These measurements served as indicators of oxidative stress.

The DAI Score

During the course of drug treatment, clinical observations included daily monitoring of mouse body weight, feces, and changes in blood in the feces.[30] Scoring was conducted according to the criteria outlined in Table 1. The Disease Activity Index (DAI) was calculated he Disease Activity Index (DAI) was calculated using the formula: DAI= (Weight Loss Score+ Fecal Consistency Score+ Blood in Feces Score)/3.

The Diarrhea Score

Diarrhea scores were monitored and assessed for severity during the experimental period, as described by Kurita et al[31] and the observations were systematically recorded daily.

Table 1 Assessment of DAI Scores

Change in Body Weight Loss	Stool Blood	Stool Consistency	Score
None	None	Normal	0
1–5%	Occult blood	Loose stool	1
5–10%	Bleeding	Loose stool	2
10–20%	Gross bleeding	Diarrhea	3
> 20%	Gross bleeding	Diarrhea	4

H&E and Pathological Scoring

After the mice were euthanized, the colon tissue was rapidly isolated, cleaned, photographed, and its length was measured. A 1 cm colon segment was collected, fixed in 4% paraformaldehyde for 24 hours, embedded in paraffin, and sectioned into 4-μm slices for hematoxylin and eosin (H&E) staining and microscopic observation. The distal colon sample was similarly processed following 48-hour fixation. Pathological scoring was performed to assess inflammatory cell infiltration, mucosal thickening, goblet cell depletion, structural damage, and crypt loss.[32]

RT-qPCR

Total RNA was isolated from colon tissue using the TRIzol reagent (Tiangen, Beijing, China). Complementary DNA (cDNA) was synthesized with the PrimeScript RT reagent kit (Perfect Real-Time, Takara, Dalian, China). Quantitative PCR was conducted on an ABI StepOne+ real-time PCR system utilizing SYBR Green PCR core reagents (Takara, Dalian, China) with primer sequences listed in Table 2. Gene expression levels were normalized to GAPDH mRNA levels, and relative expression was determined using the ΔΔCt method.

Table 2 Primer Sequences

Genes	Species	Primer Sequences (5′-3′)
TNF-α	Mouse	F: 5′-AGGCAACCACCAAGTGGAGGAG-3′ R: 5′-GCTGGGTTTGCTACGACGTGG-3′
TNF-α	Human	F: 5′-CAGAGGGAAGAGTTCCCCCAG-3′ R: 5′-CCTGGTTATCTCTCAGCTCCAC-3′
IL-1β	Mouse	F: 5′-GCAACTGTTCCTGAACTCAACT-3′ R: 5′-ATCTTTTGGGGTCCGTCAACT-3′
IL-1β	Human	F: 5′-ATGATGGCTTATTACAGTGGCAA-3′ R: 5′-GTCGGAGATTCGTAGCTGGA-3′
IL-6	Mouse	F: 5′-GTTCTCTGGGAAATCGTGGA-3′ R: 5′-TGTACTCCAGGTAGCTATGG-3′
IL-6	Human	F: 5′-AAATTCGGTACATCCTCGACGGCA-3′ R: 5′-AGTGCCTCTTTGCTGCTTTCACAC-3′
IL-10	Mouse	F: 5′-GCTCTTACTGACTGGCATGAG-3′ R: 5′-CGCAGCTCTAGGAGCATGTG-3′
IL-10	Human	F: 5′-GACTTTAAGGGTTACCTGGGTTG-3′ R: 5′-TCACATGCGCCTTGATGTCTG-3′
iNOS	Mouse	F: 5′-CAGCTGGGCTGTACAAACCTT-3′ R: 5′-CATTGGAAGTGAAGCGTTTCG-3′

(*Continued*)

Table 2 (Continued).

Genes	Species	Primer Sequences (5′-3′)
iNOS	Human	F: 5′-CCCTTCCGAAGTTTCTGGCAGCAGC-3′ R: 5′-GGCTGTCAGAGCCTCGTGGCTTTGG-3′
Cox-2	Mouse	F: 5′-GCTGGAACATGGAATTACCC-3′ R: 5′-CAGTATTGAGGAGAACAGATGGG-3′
Cox-2	Human	F: 5′-TGAAACCCACTCCAAACACAG-3′ R: 5′-TCATCAGGCACAGGAGGAAG-3′
TAK1	Mouse	F: 5′-GCTGCTGCTGCTGCTGCTG-3′ R: 5′-GCTGCTGCTGCTGCTGCTG-3′
TAK1	Human	F: 5′-GGAAGAGGAGGAGGAGGAGG-3′ R: 5′-CTGCTGCTGCTGCTGCTGC-3′
GAPDH	Mouse	F: 5′-GAGAAGGACCCGAAGAACTG-3′ R: 5′-CAGGCTTGTCCAGTAGGAGG-3′
GAPDH	Human	F: 5′-GAAGGTGAAGGTCGGAGTCA-3′ R: 5′-GACAAGCTTCCCGTTCTCAG-3′

Western Blot Analysis

Colon tissue was homogenized in RIPA lysis buffer supplemented with PMSF protease inhibitors to prevent protein degradation. Protein concentrations were determined using a BCA protein assay kit. Subsequently, 25 micrograms of protein from each sample were separated by sodium dodecyl sulfate-polyacrylamide gel electrophoresis (SDS-PAGE) and transferred onto a PVDF membrane. The membrane was incubated overnight at 4°C with primary antibodies, including ZO-1, E-cadherin, Occludin-1, TAK1, IκB-α, p- IκB-α, p65, p-p65 (all at a 1:1000 dilution), and GAPDH (at a 1:2000 dilution). Following this, the membrane was incubated with secondary antibodies at room temperature for 1.5 hours. Protein bands were visualized using an Enhanced Chemiluminescence (ECL) system and analyzed with ImageJ software.

Immunohistochemistry

The colon tissue is fixed in 10% formalin and embedded in paraffin. Sections are cut at 4 micrometers thickness, deparaffinized, and rehydrated, followed by heating in citrate buffer for antigen retrieval. The sections are blocked with 5% bovine serum albumin and subsequently incubated overnight at 4°C with primary antibodies (MUC-2, TAK1). Following this, the sections are incubated with biotinylated secondary antibodies for 30 minutes. Color development is performed using a DAB kit, with positive signals appearing as brown staining. Finally, the sections are counterstained with hematoxylin and observed under a light microscope.

Immunofluorescence

Caco-2 cells are seeded in a six-well plate containing coverslips. Once 70% confluence is reached on the coverslips, 100 ng/mL LPS is added. After 24 hours, the coverslips are collected, fixed with 4% paraformaldehyde, permeabilized, and blocked for non-specific binding. The cells are incubated overnight with TAK1 antibody, followed by incubation with a fluorescently labeled secondary antibody. The nuclei are stained with DAPI, and the coverslips are mounted with an anti-fade mounting medium before being observed under a fluorescence microscope.

Statistical Analysis

All statistical analyses were performed using SPSS 20.0 software, with graphical representations created through GraphPad Prism 9.0. Data normality was evaluated using the Shapiro–Wilk test, and experimental results were expressed

as mean ± SEM (standard error of the mean) derived from a minimum of three independent replicates. The analytical approach was tailored to data distribution patterns: Non-normally distributed datasets were analyzed using the Kruskal–Wallis nonparametric test, while normally distributed data underwent one-way ANOVA followed by Tukey's post hoc multiple comparisons test when significant intergroup differences were identified ($p<0.05$). Statistical significance was defined as $p<0.05$ for all comparisons.

Results

SSD Enhances the Anti-Tumor Effect of IRI

As shown in Figure 1A, the chemical structure of SSD is clearly depicted. Figure 1B illustrates the administration mode diagram in the mouse subcutaneous syngeneic tumor model, delineating the treatment protocols for each experimental group. We further observed that SSD exhibited a synergistic effect with IRI in inhibiting tumor growth, with the combination of H-SSD and IRI showing the strongest inhibitory effect compared to IRI monotherapy (Figure 1C). Throughout the experiment, tumor volumes and weights in the combination treatment groups were significantly smaller than those in the control group (Figure 1D and E). These results demonstrate that the combined administration of SSD and IRI can synergistically inhibit in vivo tumor growth.

SSD Alleviates IRI-Induced Intestinal Mucositis in Mice

To evaluate the protective effects of SSD on IRI-induced intestinal mucositis, the drug administration scheme is shown in Figure 2A. Mice were sacrificed on day 14, and intestinal tissues were collected. The results showed that mice treated with IRI alone exhibited weight loss, diarrhea, and rectal bleeding. Specifically, the IRI group had significantly lower body weight and DAI scores compared to the control group (Figure 2B and C). Notably, in the IRI + SSD (8 mg/kg)

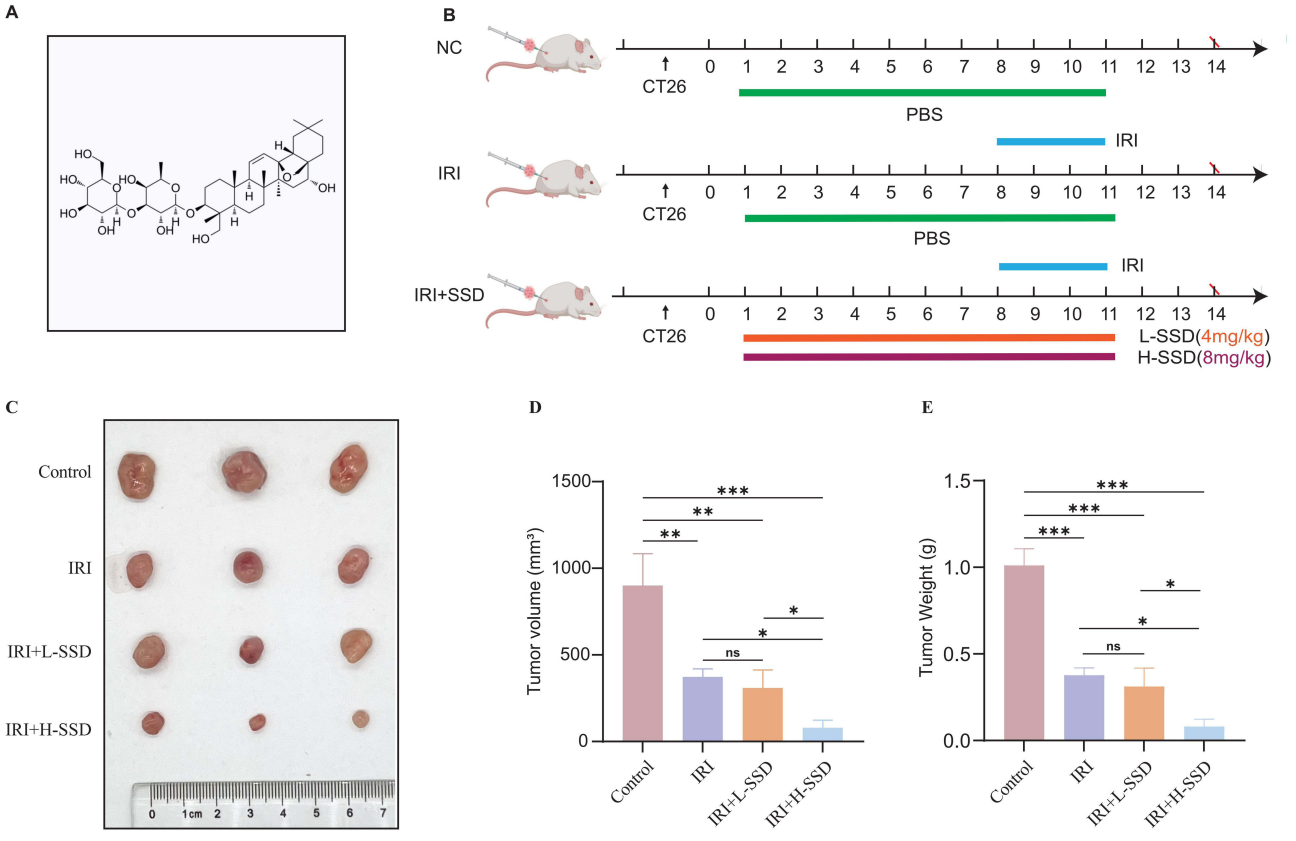

Figure 1 SSD Synergizes with IRI to Suppress Tumor Growth. (**A**) Molecular Formula. (**B**) Administration Mode Diagram in Mouse Subcutaneous Syngeneic Tumor Model. (**C**) Tumor Gross Appearance. (**D** and **E**) Tumor Volume and Weight. Data are presented as mean ± SD. *p < 0.05, **p < 0.01, ***p < 0.001, and n.s. = not significant (p > 0.05), for each group (n=3).

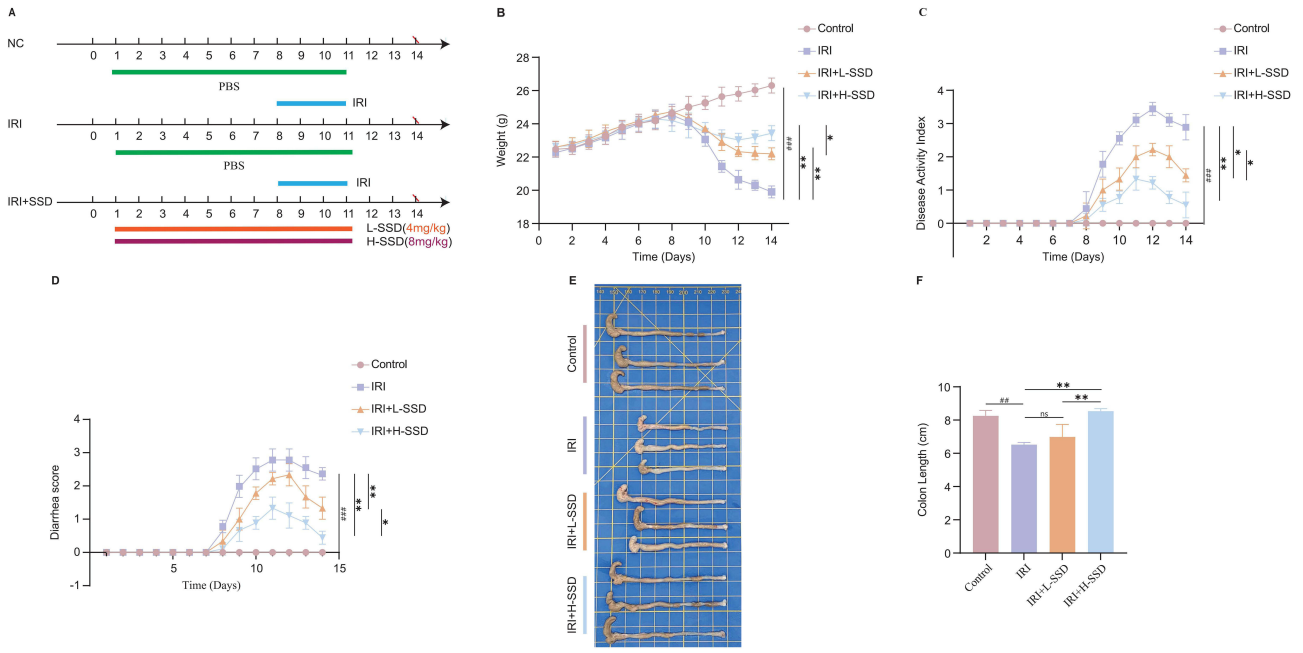

Figure 2 SSD Alleviates IRI-induced intestinal mucositis in Mice. (**A**) Schematic Diagram of IRI-Induced Mucositis Model. (**B**) Weight Trend. (**C**) Disease Activity Index (DAI). (**D**) Diarrhea Score. (**E**) Colon Morphology. (**F**) Comparison of Colon Length. Data are presented as mean ± SD. $^{\#\#}p < 0.05$, $^{\#\#\#\#}p < 0.001$ vs Control group; *p < 0.05, **p < 0.01 vs IRI group, and n.s. = not significant (p > 0.05), for each group (n=3).

group, daily SSD administration at 8 mg/kg significantly alleviated these symptoms, as evidenced by increased body weight, reduced DAI scores ($P < 0.01$), and improved diarrhea scores (Figure 2D). As an indicator of inflammatory severity, colon length measurements revealed that the IRI group had shortened colons, whereas SSD treatment in the IRI + SSD (8 mg/kg) group significantly restored colon length (Figure 2E and F). In contrast, the IRI + SSD (4 mg/kg) group showed no significant differences in colon length, compared to the IRI group. Thus, SSD at 8 mg/kg effectively alleviated IRI-induced intestinal symptoms in mice.

SSD Attenuates IRI-Induced Intestinal Epithelial Barrier Dysfunction

Pathological examination of colon tissues from healthy mice revealed normal architecture with no pathological alterations.[29] IRI treatment induced intestinal toxicity, significantly compromising the intestinal epithelial barrier function, as evidenced by inflammatory cell infiltration, mucosal thickening, reduced goblet cell numbers, and loss of crypt structures (Figure 3A). Compared to the control group, the IRI group exhibited significantly elevated pathological scores (Figure 3B). Notably, SSD (8 mg/kg) treatment markedly preserved the structural integrity of colon tissues and effectively suppressed inflammatory cell infiltration. The pathological scores in the IRI + SSD (8 mg/kg) group were significantly lower than those in the IRI group. Although low-dose SSD (4 mg/kg) also improved pathological features, its efficacy was inferior to that of high-dose SSD (8 mg/kg). Western blot analysis further demonstrated that IRI + SSD (8 mg/kg) treatment reversed the IRI-induced downregulation of intestinal barrier-associated proteins ZO-1, E-cadherin, and Occludin (Figure 3C). Additionally, immunohistochemical analysis revealed a significant reduction in MUC-2 expression levels in the colon tissues of the IRI group, indicating impaired mucus secretion and compromised intestinal barrier integrity. SSD (8 mg/kg) treatment effectively restored MUC-2 expression levels in the IRI + SSD (8 mg/kg) group (Figure 3D). In conclusion, 8 mg/kg SSD treatment demonstrated significant protective effects against IRI-induced intestinal epithelial barrier damage.

https://doi.org/10.2147/JIR.S504696

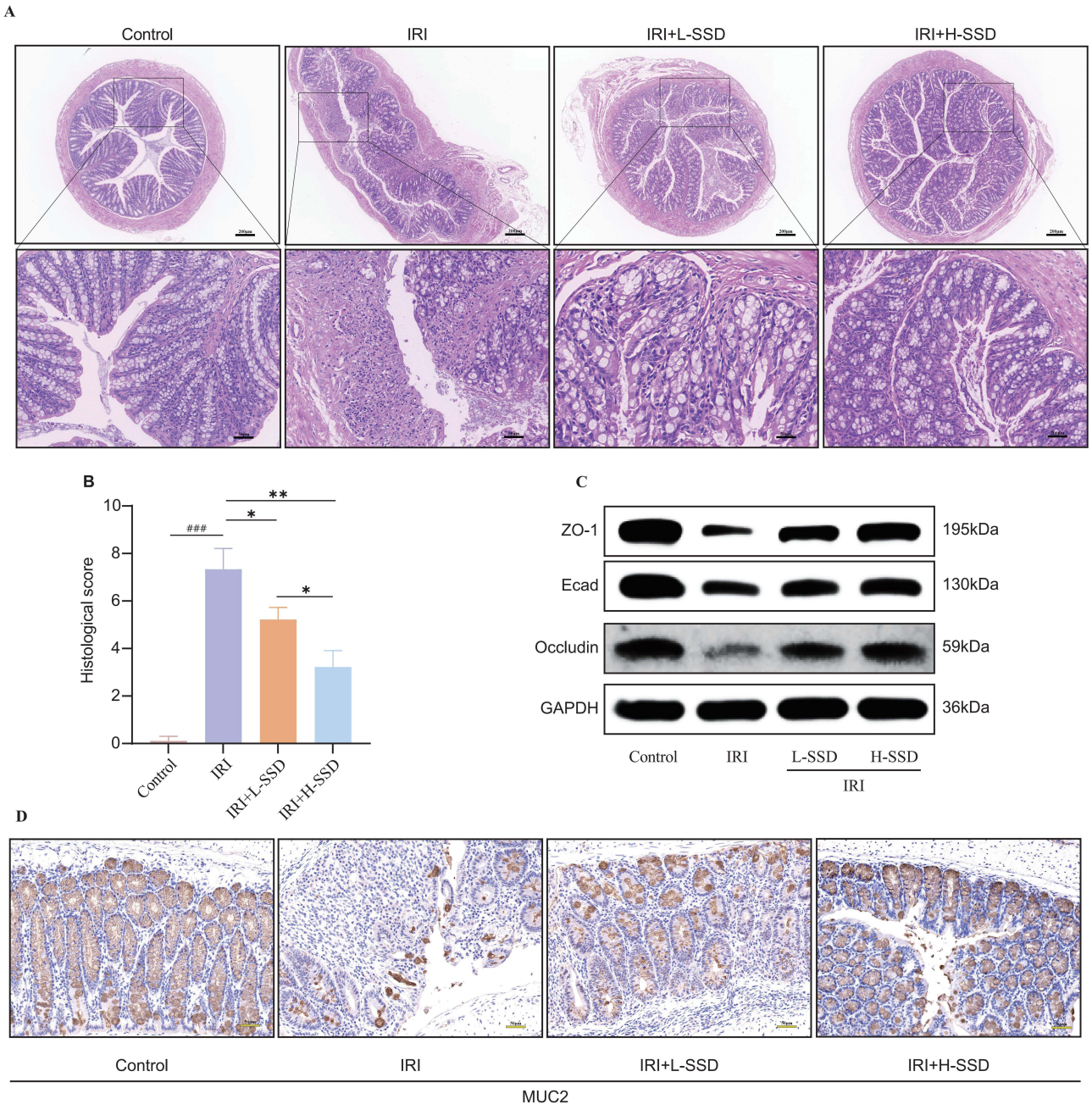

Figure 3 SSD Attenuates IRI-Induced Intestinal Epithelial Barrier Dysfunction. (**A**) Intestinal HE staining (5× Magnification and 20× Magnification). (**B**) Intestinal pathological scoring. (**C**) Western blot images of ZO-1, Occludin, E-Cadherin, and GAPDH. (**D**) MUC-2 immunohistochemistry (20× Magnification). Data are presented as mean ± SD. $^{###}p < 0.001$ vs Control group; $^{*}p < 0.05$, $^{**}p < 0.01$ vs IRI group, for each group (n=3).

SSD Inhibits Pro-Inflammatory Cytokine Production in IRI-Induced Intestinal Mucositis Mice

An imbalance in the expression of pro-inflammatory and anti-inflammatory cytokines plays a critical role in the development and progression of colitis. To investigate the regulatory effects of SSD on IRI-induced colonic inflammation in mice, we compared cytokine levels with those in normal mice. The study revealed a significant elevation in pro-inflammatory cytokines, including IL-1β, IL-6, Cox-2, iNOS, and TNF-α. Quantitative real-time PCR (q-PCR) results demonstrated that IRI treatment triggered severe inflammatory responses in mouse colonic tissues. Notably, subsequent SSD treatment effectively reduced the elevated levels of these inflammatory cytokines. As shown in Figure 4A–F, SSD

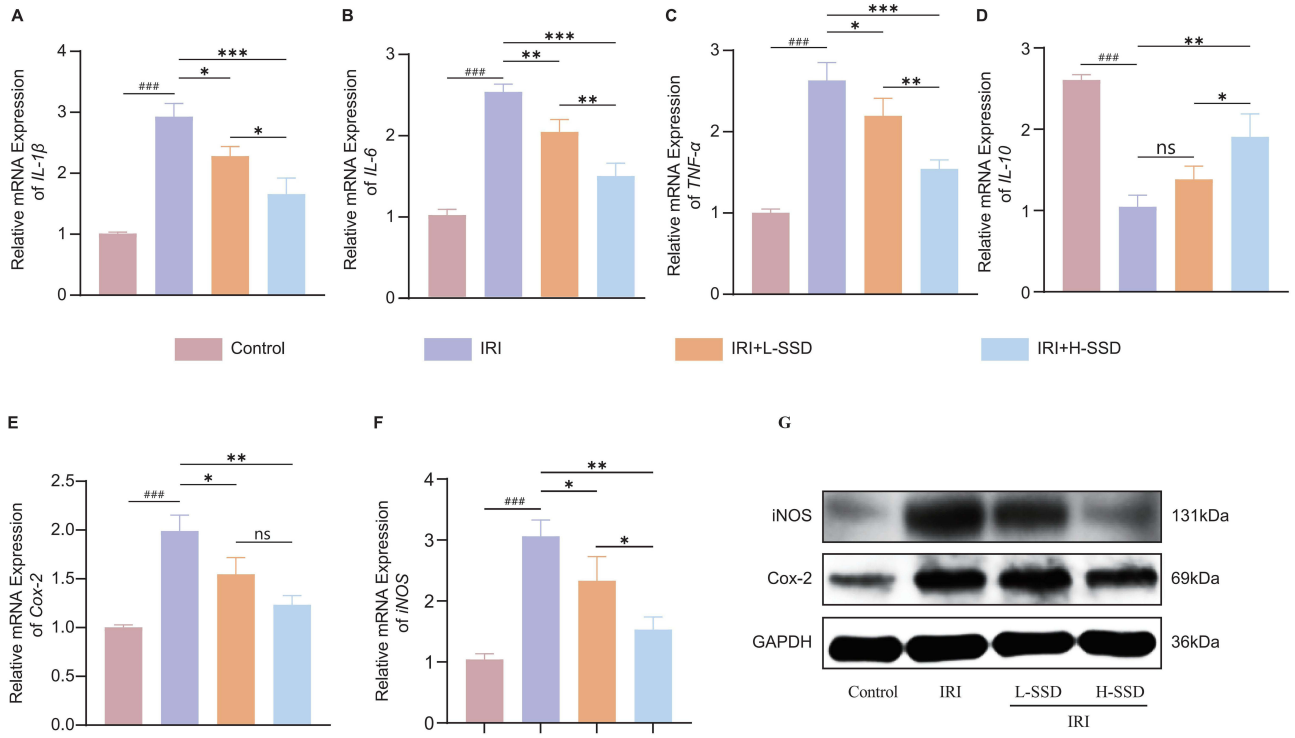

Figure 4 SSD Inhibits Pro-inflammatory Cytokine Production in IRI-induced Intestinal Mucositis Mice (**A**–**F**) mRNA Levels of IL-1β, IL-6, TNF-α, IL-10, COX-2 and iNOS. (**G**) Protein levels of COX-2 and iNOS. Data are presented as mean ± SD. ###p < 0.001 vs Control group; *p < 0.05, **p < 0.01, ***p < 0.001 vs IRI group, and n.s. = not significant (p > 0.05), for each group (n=3).

exhibited substantial therapeutic effects by significantly attenuating the abnormal increases in IL-1β, IL-6, TNF-α, Cox-2, and iNOS in colonic tissues ($p < 0.05$). Additionally, Western blot analysis of iNOS and COX-2 further corroborated this trend (Figure 4G), indicating a pronounced anti-inflammatory effect of SSD.

SSD Enhances Antioxidant Capacity in IRI-Induced Intestinal Mucositis Mice

Given the close association between oxidative stress and inflammation, antioxidants may serve as a preventive strategy for inflammatory diseases.[33] By analyzing the activities of glutathione peroxidase (GSH-PX), superoxide dismutase (SOD), and myeloperoxidase (MPO), as well as the level of malondialdehyde (MDA), we assessed the antioxidant status of colon tissue samples. As shown in Figure 5A and B, after IRI treatment, the activity of GSH-PX in the supernatant of mouse colon tissue was significantly reduced, while MDA levels increased. SSD treatment significantly reversed the decline in the activity of these oxidative enzymes. Additionally, SOD, a commonly used marker for evaluating neutrophil function and activity in inflamed tissues,[34] showed significantly lower levels in the IRI-treated group compared to mice treated with SSD (4 mg/kg or 8 mg/kg). Furthermore, we evaluated the antioxidant effects of SSD using MPO, another oxidative stress marker (Figure 5C and D). Compared to control mice, IRI treatment significantly elevated MPO levels, whereas SSD treatment reduced the elevated MPO levels. These results indicate that SSD enhances the antioxidant capacity in IRI-induced intestinal mucositis.

SSD Alleviates IRI-Induced Intestinal Mucositis Mice via the TAK1/NF-kB Pathway

To further investigate the mechanism of action of SSD, we focused on the TAK1/NF-κB signaling pathway, a key inflammatory pathway. First, we examined the mRNA levels of TAK1 in colonic tissue to analyze the relevant regulatory mechanisms. As shown in Figure 6A, treatment with IRI significantly increased the mRNA levels of TAK1 compared to the control group, while SSD effectively reduced its expression. Western blotting and Immunohistochemistry results also demonstrated a similar trend (Figure 6B and C). Additionally, the statistical analysis graph for TAK1 protein expression has been added to (Supplementary Figure 1). As an upstream regulator of the NF-κB signaling pathway, we hypothesized

https://doi.org/10.2147/JIR.S504696

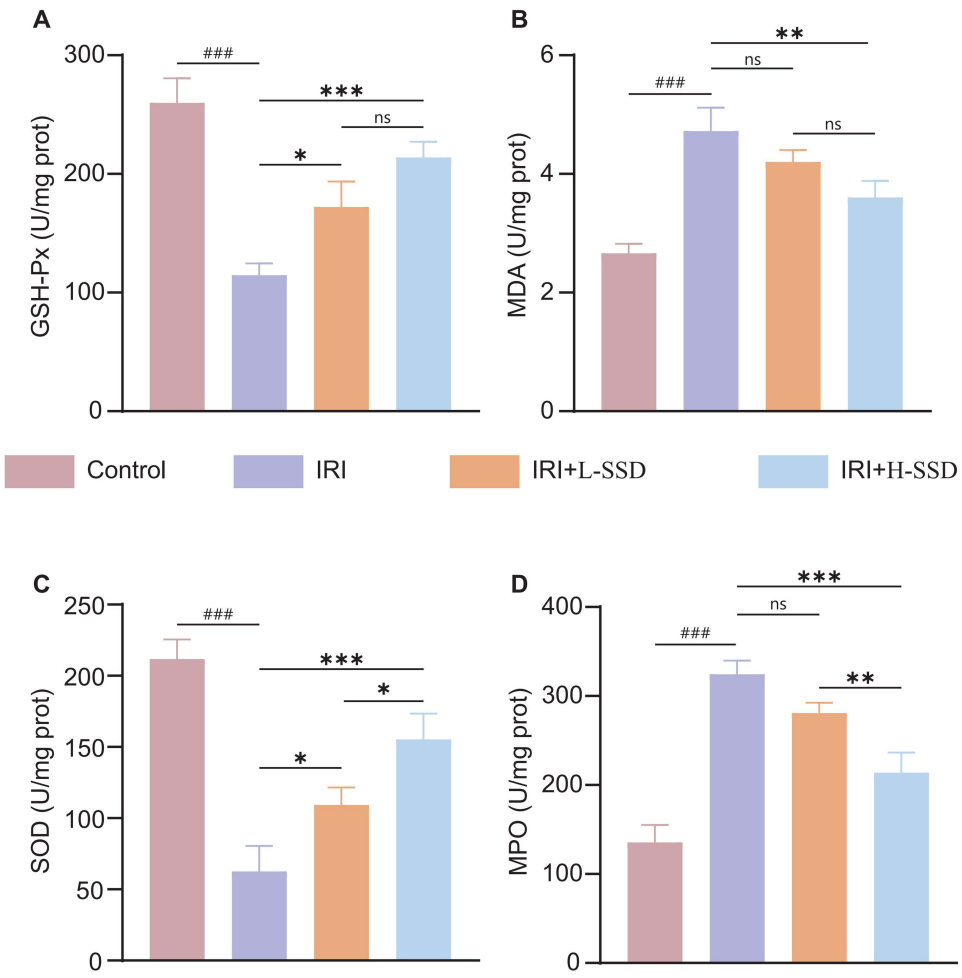

Figure 5 3.5 SSD Enhances Antioxidant Capacity in IRI-induced Intestinal Mucositis Mice. (**A**–**D**) The activities of oxidative stress markers, including GSH-Px, MDA, SOD and MPO (**A**–**D**). Data are presented as mean ± SD. $^{###}p < 0.001$ vs Control group; $^{*}p < 0.05$, $^{**}p < 0.01$, $^{***}p < 0.001$ vs IRI group, and n.s. = not significant ($p > 0.05$), for each group (n=3).

that TAK1 may exert its anti-inflammatory effects by inhibiting the activation of NF-κB. Subsequently, we utilized Western blotting to detect the levels of p-p65/p65 and p-IκB-α/IκB-α, and found that the levels of p-p65 and p-IκB-α proteins were significantly increased in the IRI group compared to the control group. However, treatment with SSD significantly reduced the expression levels of these proteins (Figure 6D and G). These results indicate that SSD influences the activation of the NF-κB pathway by regulating TAK1 expression, thereby exerting its anti-inflammatory effects.

SSD Alleviates LPS-Induced Cellular Inflammation via the TAK1/NF-kB Pathway

To evaluate the anti-inflammatory effects of SSD, this study systematically investigated using a Caco-2 cell model. The CCK-8 assay revealed that varying concentrations of SSD (1–40 μM) exhibited no significant cytotoxicity (Figure 7A), leading to the selection of 2.5 μM and 5 μM for subsequent experiments. In the LPS-induced inflammatory model of Caco-2 cells, SSD treatment significantly suppressed the secretion of pro-inflammatory cytokines IL-1β, IL-6, and TNF-α (Figure 7B–D), while upregulating the expression of anti-inflammatory cytokine IL-10 (Figure 7E). Western blot analysis revealed dose-dependent suppression of pro-inflammatory mediators iNOS and COX-2 protein expression by SSD (Figure 7F), with quantitative band intensity analysis provided in (Supplementary Figure 2). Mechanistic studies indicated that SSD exerts its anti-inflammatory effects by regulating the TAK1/NF-κB signaling pathway. qPCR and immunofluorescence results showed that SSD treatment significantly downregulated TAK1 mRNA expression

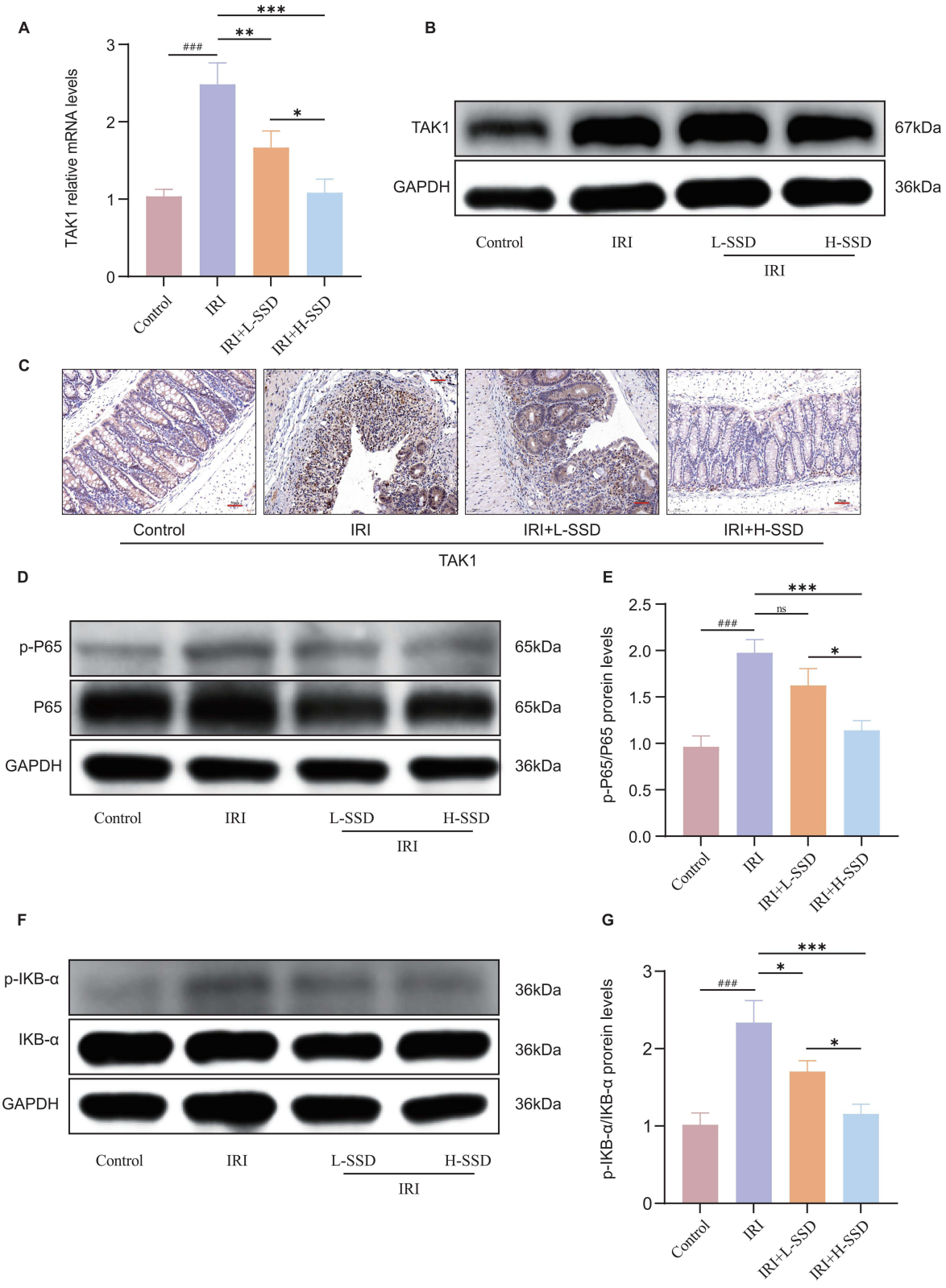

Figure 6 SSD Alleviates IRI-induced Intestinal Mucositis Mice via the TAK1/NF-kB Pathway. (**A**) mRNA levels of TAK1. (**B**) Protein levels of TAK1. (**C**) Immunohistochemistry of TAK1 (20× Magnification). (**D** and **E**) Western blot analysis of the colon tissue (GAPDH, p65, p-p65). (**F** and **G**) Western blot analysis of the colon tissue (GAPDH, IkB-α, p-IkB-α). Data are presented as mean ± SD. ###p < 0.001 vs Control group; *p < 0.05, **p < 0.01, ***p < 0.001 vs IRI group, and n.s. = not significant (p > 0.05), for each group (n=3).

https://doi.org/10.2147/JIR.S504696

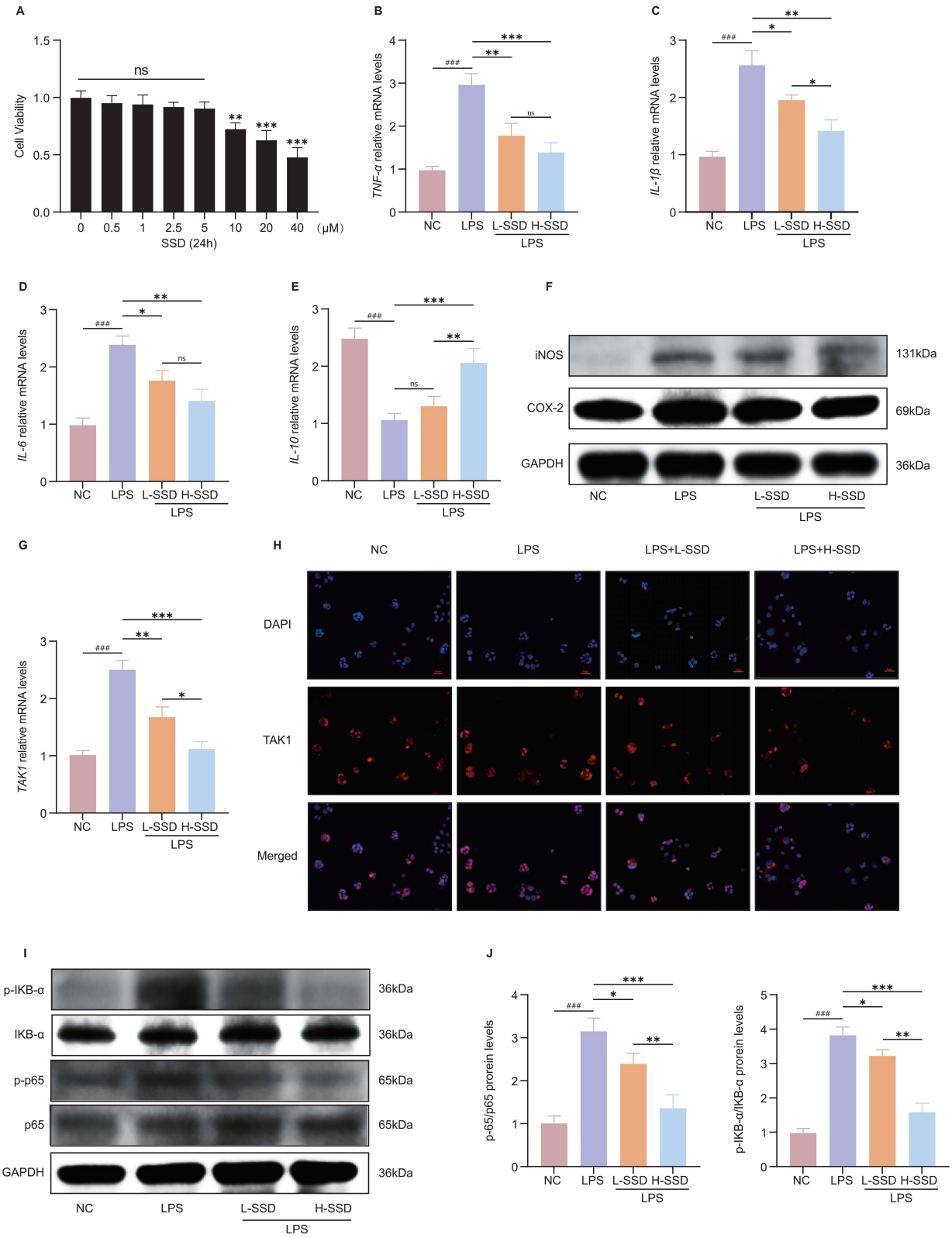

Figure 7 SSD Alleviates LPS-Induced Cellular Inflammation via the TAK1/NF-kB Pathway. (**A**) CCK8. (**B–E**) q-PCR Detection of IL-1β, IL-6, IL-10, and TNF-α Levels. (**F**) Protein levels of COX-2 and iNOS. (**G** and **H**) mRNA levels of TAK1. (**H**) Immunofluorescence of TAK1 molecules in Caco-2 cells (20× Magnification). (**I** and **J**) Protein levels and quantitative statistics of p-p65, p65, IκB-α, and p-IκB-α. Data are presented as mean ± SD. $^{###}p < 0.001$ vs Control group; $^{*}p < 0.05$, $^{**}p < 0.01$, $^{***}p < 0.001$ vs LPS group, and n.s. = not significant ($p > 0.05$), for each group (n=3).

(Figure 7G) and altered its protein localization (Figure 7H). Western blot analysis confirmed that SSD inhibited the phosphorylation levels of key NF-κB pathway proteins p-p65 and p-IκB-α (Figure 7I and J), consistent with in vivo experimental data. In conclusion, this study reveals that SSD suppresses LPS-induced inflammatory responses through targeted modulation of the TAK1/NF-κB signaling pathway.

Discussion

Chemotherapy-induced side effects are prevalent in clinical practice and significantly impact patients' quality of life. Traditional Chinese Medicine plays a crucial role as an adjunct therapy during postoperative, radiotherapy, and chemotherapy periods. Various Chinese herbal medicines, such as Berberine,[35] ginseng,[36] and Curcumin,[37] have been shown to have notable effects in alleviating discomfort associated with cancer. IRI treatment is often accompanied by severe gastrointestinal toxicity, manifested as diarrhea and rectal bleeding, which poses a significant challenge to patients' chemotherapy tolerance.[38] Additionally, IRI may induce enteric mucositis, leading to structural damage to the intestinal lining, further reducing patients' chemotherapy tolerance and adversely affecting tumor treatment efficacy.

SSD has been reported to exhibit anti-inflammatory, antitumor, and antiviral effects in various disease models; however, its potential for preventing and treating IRI-induced intestinal toxicity has not been explored. Based on preliminary animal experiments, we confirmed the preventive and protective effects of SSD on IRI-induced intestinal mucositis in a mouse model. As shown in Figure 2, SSD treatment significantly reduced the incidence of intestinal mucositis and was accompanied by increased body weight in mice. Furthermore, the protective effects of SSD extend beyond alleviating intestinal mucositis, demonstrating efficacy in mitigating mucosal damage and ameliorating intestinal barrier dysfunction. Previous studies have indicated that IRI treatment directly compromises the integrity of the mucosal barrier and intestinal epithelial cells.[15] In this study, administration of SSD (8 mg/kg) significantly upregulated the protein expression levels of Muc2, ECAD, Claudin-1, and ZO-1.

To investigate the effects of SSD on inflammatory responses, this study analyzed the mRNA expression levels of TNF-α, IL-6, IL-1β, and IL-10 in colon tissue. Consistent with previous findings,[4,39] we observed elevated mRNA levels of TNF-α, IL-6, and IL-1β in the colonic tissues of IRI-induced mice. However, treatment with SSD significantly reduced the expression of these pro-inflammatory cytokines, including IL-1β, TNF-α, COX-2, and IL-6 (Figure 4), thereby alleviating the severity of mucosal inflammation and maintaining intestinal integrity. Inflammation is closely associated with oxidative stress, and previous studies have demonstrated that pro-inflammatory cytokines can induce oxidative stress by promoting reactive oxygen species (ROS) production in immune cells.[40,41] Building on this evidence and our observed accumulation of pro-inflammatory cytokines, we hypothesize that SSD may exert therapeutic effects through enhancement of the body's antioxidant capacity. The results showed that IRI treatment significantly increased oxidative stress markers in the colons of model mice (Figure 5). Following SSD co-intervention, GSH-Px and SOD activities were significantly elevated, while MDA and MOP levels markedly decreased, demonstrating SSD's potent antioxidant capacity in irinotecan-induced intestinal mucositis.(The original version)

IRI treatment significantly increased oxidative stress markers in the colons of model mice, but subsequent co-intervention with SSD led to significant elevations in GSH-Px and SOD activities, along with marked decreases in MDA and MOP levels (Figure 5). This finding demonstrates SSD's potent antioxidant capacity in irinotecan-induced intestinal mucositis.(The revised version)

Our findings reveal that SSD exhibits anti-inflammatory effects in LPS-induced RAW264.7 cells, primarily through the inhibition of NF-kB activation and the subsequent production of pro-inflammatory cytokines.[42] LPS stimulation leads to the phosphorylation of IkB-α, which facilitates the translocation of NF-kB from the cytoplasm to the nucleus, thereby activating the NF-kB signaling pathway. Notably, NF-kB is recognized as a central component of the inflammatory response. Abnormal activation of NF-kB triggers inflammatory responses, leading to an imbalance between pro-inflammatory and anti-inflammatory cytokines.[43] This imbalance is characterized by an increase in the release of pro-inflammatory cytokines such as TNF-α, IL-1β, and IL-6, while the secretion of IL-10 is suppressed. In this study, consistent changes in these cytokines were observed in IRI-induced mice. Therefore, targeting the NF-kB pathway is particularly used in the treatment of inflammation-related enteritis, especially chemotherapy-induced enteritis. Interestingly, the findings of this study reveal that treatment with 8 mg/kg SSD effectively inhibits NF-kB pathway

activation by reducing the levels of p-IkB-α protein in the colons of mice. The activation of NF-kB and its associated pathways is triggered by various pro-inflammatory cytokines, which further exacerbate the inflammatory response, a phenomenon that has been extensively documented in the literature.[44] However, research on TAK1 in the context of chemotherapy-induced intestinal toxicity remains limited. TAK1, a serine/threonine kinase, serves as a crucial upstream regulator of multiple inflammation-related signaling pathways. Previous studies have identified TAK1 as a promising therapeutic target for ulcerative colitis (UC).[45] TAK1 inhibitors have been shown to effectively suppress downstream inflammation-related signaling pathways, thereby downregulating the expression of inflammatory mediators and extracellular matrix components.[46]

This study demonstrates that SSD may exert its anti-inflammatory and mucosal protective effects through modulation of the TAK1/NF-κB signaling pathway, providing an important theoretical foundation for developing novel therapeutic strategies for intestinal inflammation. Notably, SSD exhibits a dose-dependent safety profile (8 mg/kg) while improving intestinal barrier function, suggesting its potential for clinical translation, particularly in the prevention and treatment of mucosal barrier injury-related diseases such as chemotherapy-induced enteritis and inflammatory bowel disease (IBD). However, this study has certain limitations: First, the experimental data were derived solely from murine models, lacking validation with human tissue samples; second, the long-term toxicity of SSD and its pharmacokinetic profile in complex pathological microenvironments require systematic evaluation. Future research should focus on establishing humanized organoid models to validate cross-species mechanistic consistency and exploring synergistic effects between SSD and other mucosal repair therapies, thereby accelerating clinical translation.

Conclusion

This study demonstrated through a syngeneic transplanted tumor mouse model that the combined application of SSD and IRI synergistically inhibits colorectal tumor growth. Notably, SSD significantly alleviated IRI-induced intestinal mucositis, with its mechanism involving the protection of both structural integrity and functional maintenance of the intestinal epithelial mucosal barrier. Specifically, SSD exerted anti-inflammatory and antioxidant effects by targeting the TAK1/NF-κB signaling pathway. In vitro experiments further revealed that SSD markedly reduced the expression of inflammatory factors in LPS-induced Caco-2 cells through blocking the activation of the TAK1/NF-κB pathway. These findings highlight the clinical translational value of SSD in preventing and treating chemotherapy-associated intestinal toxicity. Future clinical trials are warranted to validate its efficacy and safety, thereby facilitating its translational application as an adjuvant therapy in cancer chemotherapy.

Abbreviations

SSD, Saikosaponin-d; IRI, Irinotecan; DAI, Disease Activity Index; MPO, myeloperoxidase; SOD, superoxide dismutase; GSH-Px, glutathione peroxidase; MDA, malondialdehyde; UC, ulcerative colitis; IBD, inflammatory bowel disease.

Acknowledgments

We would like to express our gratitude to everyone who contributed to this study. Special thanks to our research team for their dedication and hard work. We also appreciate the support from our funding agencies, which provided essential resources.

Funding

There is no funding to report.

Disclosure

The authors report no conflicts of interest in this work.

References

1. Colvin LA. Chemotherapy-induced peripheral neuropathy: where are we now? *Pain*. 2019;160(Suppl 1):S1–S10. doi:10.1097/j.pain.0000000000001540

2. Abdel-Razeq H, Hashem H. Recent update in the pathogenesis and treatment of chemotherapy and cancer induced anemia. *Crit Rev Oncol Hematol*. 2020;145:102837. doi:10.1016/j.critrevonc.2019.102837
3. Cheng L, Li M, Hu J, et al. UGT1A1*6 polymorphisms are correlated with irinotecan-induced toxicity: a system review and meta-analysis in Asians. *Cancer Chemother Pharmacol*. 2014;73(3):551–560. doi:10.1007/s00280-014-2382-3
4. Wu Y, Wang D, Yang X, Fu C, Zou L, Zhang J. Traditional Chinese medicine Gegen Qinlian decoction ameliorates irinotecan chemotherapy-induced gut toxicity in mice. *Biomed Pharmacother*. 2019;109:2252–2261. doi:10.1016/j.biopha.2018.11.095
5. Campbell JM, Stephenson MD, Bateman E, Peters MD, Keefe DM, Bowen JM. Irinotecan-induced toxicity pharmacogenetics: an umbrella review of systematic reviews and meta-analyses. *Pharmacogenomics J*. 2017;17(1):21–28. doi:10.1038/tpj.2016.58
6. Chen YJ, Hu F, Li CY, et al. The association of UGT1A1*6 and UGT1A1*28 with irinotecan-induced neutropenia in Asians: a meta-analysis. *Biomarkers*. 2014;19(1):56–62. doi:10.3109/1354750X.2013.867534
7. Wardill HR, Gibson RJ, Van Sebille YZ, et al. Irinotecan-induced gastrointestinal dysfunction and pain are mediated by common TLR4-dependent mechanisms. *Mol Cancer Ther*. 2016;15(6):1376–1386. doi:10.1158/1535-7163.MCT-15-0990
8. Chamseddine AN, Ducreux M, Armand JP, et al. Intestinal bacterial beta-glucuronidase as a possible predictive biomarker of irinotecan-induced diarrhea severity. *Pharmacol Ther*. 2019;199:1–15. doi:10.1016/j.pharmthera.2019.03.002
9. Mego M, Chovanec J, Vochyanova-Andrezalova I, et al. Prevention of irinotecan induced diarrhea by probiotics: a randomized double blind, placebo controlled pilot study. *Complement Ther Med*. 2015;23(3):356–362. doi:10.1016/j.ctim.2015.03.008
10. Huang H, Wang X, Zhang X, et al. Ganciclovir reduces irinotecan-induced intestinal toxicity by inhibiting NLRP3 activation. *Cancer Chemother Pharmacol*. 2020;85(1):195–204. doi:10.1007/s00280-019-03996-y
11. Arimori K, Kuroki N, Hidaka M, et al. Effect of P-glycoprotein modulator, cyclosporin A, on the gastrointestinal excretion of irinotecan and its metabolite SN-38 in rats. *Pharm Res*. 2003;20(6):910–917. doi:10.1023/a:1023847521767
12. Yang XX, Hu ZP, Xu AL, et al. A mechanistic study on reduced toxicity of irinotecan by coadministered thalidomide, a tumor necrosis factor-alpha inhibitor. *J Pharmacol Exp Ther*. 2006;319(1):82–104. doi:10.1124/jpet.106.103606
13. Qi F, Li A, Inagaki Y, et al. Chinese herbal medicines as adjuvant treatment during chemo- or radio-therapy for cancer. *Biosci Trends*. 2010;4(6):297–307.
14. Zhang X, Qiu H, Li C, Cai P, Qi F. The positive role of traditional Chinese medicine as an adjunctive therapy for cancer. *Biosci Trends*. 2021;15(5):283–298. doi:10.5582/bst.2021.01318
15. Jia HJ, Rui Bai S, Xia J, et al. Artesunate ameliorates irinotecan-induced intestinal injury by suppressing cellular senescence and significantly enhances anti-tumor activity. *Int Immunopharmacol*. 2023;119:110205. doi:10.1016/j.intimp.2023.110205
16. Bui TT, Piao CH, Hyeon E, et al. Preventive effect of Bupleurum chinense on nasal inflammation via suppressing T helper type 2, eosinophil and mast cell activation. *Am J Chin Med*. 2019;47(2):405–421. doi:10.1142/S0192415X19500204
17. Kang Y, Gao Y, Li X, et al. Bupleurum chinense exerts a mild antipyretic effect on LPS-induced pyrexia rats involving inhibition of peripheral TNF-alpha production. *J Ethnopharmacol*. 2023;310:116375. doi:10.1016/j.jep.2023.116375
18. Teng L, Guo X, Ma Y, Xu L, Wei J, Xiao P. A comprehensive review on traditional and modern research of the genus Bupleurum (Bupleurum L. Apiaceae) in recent 10 years. *J Ethnopharmacol*. 2023;306:116129. doi:10.1016/j.jep.2022.116129
19. Manoharan S, Deivendran B, Perumal E. Chemotherapeutic Potential of Saikosaponin D: experimental evidence. *J Xenobiot*. 2022;12(4):378–405. doi:10.3390/jox12040027
20. Zhou P, Shi W, He XY, Du QY, Wang F, Guo J. Saikosaponin D: review on the antitumour effects, toxicity and pharmacokinetics. *Pharm Biol*. 2021;59(1):1480–1489. doi:10.1080/13880209.2021.1992448
21. Gao T, Wang T, Wu L, et al. Saikosaponin-d alleviates depression by promoting NLRP3 ubiquitination and inhibiting inflammasome activation. *Int Immunopharmacol*. 2024;127:111324. doi:10.1016/j.intimp.2023.111324
22. Qi X, Fan M, Huang N, et al. Saikosaponin d contributed to cancer chemotherapy induced neutropenia therapy by promoting neutrophil differentiation via activation CBL-dependent ERK pathway. *Pharmacol Res*. 2020;160:105149. doi:10.1016/j.phrs.2020.105149
23. Wang HW, Liu M, Zhong TD, Fang XM. Saikosaponin-d attenuates ventilator-induced lung injury in rats. *Int J Clin Exp Med*. 2015;8(9):15137–15145.
24. Wong VK, Zhang MM, Zhou H, et al. Saikosaponin-d enhances the anticancer potency of TNF-alpha via overcoming its undesirable response of activating NF-Kappa B signalling in cancer cells. *Evid Based Complement Alternat Med*. 2013;2013:745295. doi:10.1155/2013/745295
25. Ma X, Dang C, Kang H, et al. Saikosaponin-D reduces cisplatin-induced nephrotoxicity by repressing ROS-mediated activation of MAPK and NF-kappaB signalling pathways. *Int Immunopharmacol*. 2015;28(1):399–408. doi:10.1016/j.intimp.2015.06.020
26. Chen Q, Wu S, Wu Y, Chen L, Pang Q. MiR-149 suppresses the inflammatory response of chondrocytes in osteoarthritis by down-regulating the activation of TAK1/NF-kappaB. *Biomed Pharmacother*. 2018;101:763–768. doi:10.1016/j.biopha.2018.02.133
27. Gupta P, Makkar TK, Goel L, Pahuja M. Role of inflammation and oxidative stress in chemotherapy-induced neurotoxicity. *Immunol Res*. 2022;70(6):725–741. doi:10.1007/s12026-022-09307-7
28. Lu DX, Liu F, Wu H, et al. Wumei pills attenuates 5-fluorouracil-induced intestinal mucositis through Toll-like receptor 4/myeloid differentiation factor 88/nuclear factor-kappaB pathway and microbiota regulation. *World J Gastroenterol*. 2022;28(32):4574–4599. doi:10.3748/wjg.v28.i32.4574
29. Li P, Wu M, Xiong W, et al. Saikosaponin-d ameliorates dextran sulfate sodium-induced colitis by suppressing NF-kappaB activation and modulating the gut microbiota in mice. *Int Immunopharmacol*. 2020;81:106288. doi:10.1016/j.intimp.2020.106288
30. Murthy SN, Cooper HS, Shim H, Shah RS, Ibrahim SA, Sedergran DJ. Treatment of dextran sulfate sodium-induced murine colitis by intracolonic cyclosporin. *Dig Dis Sci*. 1993;38(9):1722–1734. doi:10.1007/BF01303184
31. Kurita A, Kado S, Kaneda N, Onoue M, Hashimoto S, Yokokura T. Modified irinotecan hydrochloride (CPT-11) administration schedule improves induction of delayed-onset diarrhea in rats. *Cancer Chemother Pharmacol*. 2000;46(3):211–220. doi:10.1007/s002800000151
32. Rachmilewitz D, Karmeli F, Takabayashi K, et al. Immunostimulatory DNA ameliorates experimental and spontaneous murine colitis. *Gastroenterology*. 2002;122(5):1428–1441. doi:10.1053/gast.2002.32994
33. Yao J, Cao X, Zhang R, et al. Protective effect of baicalin against experimental colitis via suppression of oxidant stress and apoptosis. *Pharmacogn Mag*. 2016;12(47):225–234. doi:10.4103/0973-1296.186342
34. Yu CM, Wang Y, Ren SC, et al. Caffeic acid modulates activation of neutrophils and attenuates sepsis-induced organ injury by inhibiting 5-LOX/LTB4 pathway. *Int Immunopharmacol*. 2023;125(Pt A):111143. doi:10.1016/j.intimp.2023.111143

35. Devarajan N, Jayaraman S, Mahendra J, et al. Berberine-A potent chemosensitizer and chemoprotector to conventional cancer therapies. *Phytother Res*. 2021;35(6):3059–3077. doi:10.1002/ptr.7032
36. Zhao L, Zhang Y, Li Y, et al. Therapeutic effects of ginseng and ginsenosides on colorectal cancer. *Food Funct*. 2022;13(12):6450–6466. doi:10.1039/d2fo00899h
37. Weng W, Goel A. Curcumin and colorectal cancer: an update and current perspective on this natural medicine. *Semin Cancer Biol*. 2022;80:73–86. doi:10.1016/j.semcancer.2020.02.011
38. Bailly C. Irinotecan: 25 years of cancer treatment. *Pharmacol Res*. 2019;148:104398. doi:10.1016/j.phrs.2019.104398
39. Gibbons RD, Clark DC, VonAmmon Cavanaugh S, Davis JM. Application of modern psychometric theory in psychiatric research. *J Psychiatr Res*. 1985;19(1):43–55. doi:10.1016/0022-3956(85)90067-6
40. McGarry T, Biniecka M, Veale DJ, Fearon U. Hypoxia, oxidative stress and inflammation. *Free Radic Biol Med*. 2018;125:15–24. doi:10.1016/j.freeradbiomed.2018.03.042
41. Jeon YD, Lee JH, Lee YM, Kim DK. Puerarin inhibits inflammation and oxidative stress in dextran sulfate sodium-induced colitis mice model. *Biomed Pharmacother*. 2020;124:109847. doi:10.1016/j.biopha.2020.109847
42. Lu CN, Yuan ZG, Zhang XL, et al. Saikosaponin a and its epimer saikosaponin d exhibit anti-inflammatory activity by suppressing activation of NF-kappaB signaling pathway. *Int Immunopharmacol*. 2012;14(1):121–126. doi:10.1016/j.intimp.2012.06.010
43. Li B, Hu Y, Chen Y, et al. Homoplantaginin alleviates intervertebral disc degeneration by blocking the NF-kappaB/MAPK pathways via binding to TAK1. *Biochem Pharmacol*. 2024;226:116389. doi:10.1016/j.bcp.2024.116389
44. Lawrence T. The nuclear factor NF-kappaB pathway in inflammation. *Cold Spring Harb Perspect Biol*. 2009;1(6):a001651. doi:10.1101/cshperspect.a001651
45. He J, Liu L, Liu X, et al. Epoxymicheliolide prevents dextran sulfate sodium-induced colitis in mice by inhibiting TAK1-NF-kappaB pathway and activating Keap1-NRF2 signaling in macrophages. *Int Immunopharmacol*. 2022;113(Pt A):109404. doi:10.1016/j.intimp.2022.109404
46. Klatt AR, Klinger G, Neumuller O, et al. TAK1 downregulation reduces IL-1beta induced expression of MMP13, MMP1 and TNF-alpha. *Biomed Pharmacother*. 2006;60(2):55–61. doi:10.1016/j.biopha.2005.08.007